AD-A172 293 PASSIVITY MECHANISMS IN STAINLESS STEELS· MO-N SYNERGISM(U) STATE UNIV OF NEW YORK AT STONY BROOK DEPT OF MATERIALS SCIENCE AND ENGINEERING C R CLAYTON 1/1

UNCLASSIFIED AUG 86 N00014-85-K-0437 F/G 11/6 NL

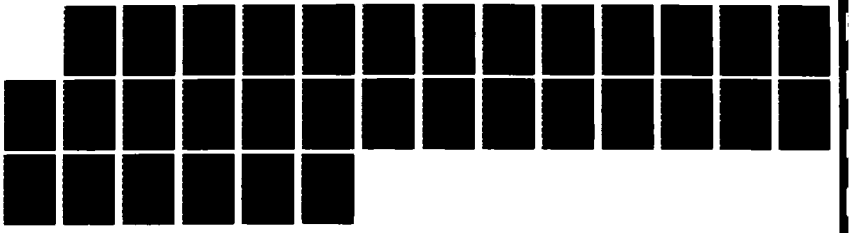

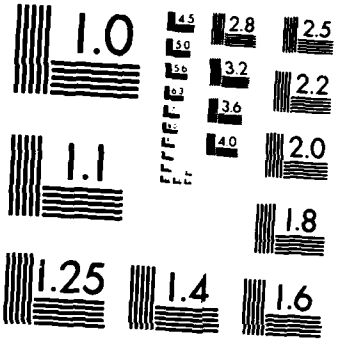

PASSIVITY MECHANISMS IN STAINLESS STEELS: Mo-N SYNERGISM

End of Year Report
August 1986

Office of Naval Research
Contract N00014-85-K-0437

Clive R. Clayton

State University of New York at Stony Brook
Dept. of Materials Science and Engineering
Stony Brook, N.Y. 11794

State University of New York at StonyBrook

Department of Materials Science and Engineering

(12)

PASSIVITY MECHANISMS IN STAINLESS STEELS:

Mo-N SYNERGISM

End of Year Report
August 1986

Office of Naval Research
Contract N00014-85-K-0437

Clive R. Clayton

State University of New York at Stony Brook
Dept. of Materials Science and Engineering
Stony Brook, N.Y. 11794

Unclassified

SECURITY CLASSIFICATION OF THIS PAGE (When Data Entered)

REPORT DOCUMENTATION PAGE		READ INSTRUCTIONS BEFORE COMPLETING FORM
1. REPORT NUMBER	2. GOVT ACCESSION NO. AD-A172293	3. RECIPIENT'S CATALOG NUMBER
4. TITLE (and Subtitle) Passivity Mechanisms in Stainless Steels: Mo-N Synergism		5. TYPE OF REPORT & PERIOD COVERED End of Year Report June 1985-June 1986
		6. PERFORMING ORG. REPORT NUMBER
7. AUTHOR(s) Clive R. Clayton		8. CONTRACT OR GRANT NUMBER(s) N00014-85-K-0437
9. PERFORMING ORGANIZATION NAME AND ADDRESS Dept. of Materials Science and Engineering State University of New York at Stony Brook Stony Brook, N.Y. 11794		10. PROGRAM ELEMENT, PROJECT, TASK AREA & WORK UNIT NUMBERS
11. CONTROLLING OFFICE NAME AND ADDRESS Office of Naval Research, Materials Division, 800 N. Quincy St., Arlington, VA		12. REPORT DATE August 1986
		13. NUMBER OF PAGES 26
14. MONITORING AGENCY NAME & ADDRESS(if different from Controlling Office)		15. SECURITY CLASS. (of this report) Unclassified
		15a. DECLASSIFICATION/DOWNGRADING SCHEDULE

16. DISTRIBUTION STATEMENT (of this Report)

This document is unclassified. Reproduction and distribution is permitted for any purpose of the U.S. Government.

17. DISTRIBUTION STATEMENT (of the abstract entered in Block 20, if different from Report)

18. SUPPLEMENTARY NOTES

19. KEY WORDS (Continue on reverse side if necessary and identify by block number)

Stainless steel	Repassivation
Nitrogen	Pitting
Passivity	Variable angle XPS

20. ABSTRACT (Continue on reverse side if necessary and identify by block number)

see reverse side

DD FORM 1 JAN 73 1473 EDITION OF 1 NOV 65 IS OBSOLETE S/N 0102-LF-014-6601

Unclassified

SECURITY CLASSIFICATION OF THIS PAGE (When Data Entered)

ABSTRACT

Increasing the N content of a commercial grade 18-8 Stainless steel from 0.04% to 0.24% N was found to raise the breakdown potential from 200 mV to 304 mV in deaerated 0.1M HCl (pH 1.2). In deaerated 0.5M H_2SO_4 + 0.5M NaCl (pH 0.4) the 0.04% N alloy pitted at 448 mV. The 0.24% N alloy exhibited breakdown at 448 mV, a pitting inhibition potential at 540 mV, and a final pitting potential at 640 mV. Variable angle XPS studies of the passive film formed on the 0.24% N alloy at 0 mV after 10 seconds and 1 hour provided evidence of the role of N and SO_4^{2-} in the initial stages of repassivation. The N was found to exist in three forms, namely CrN (397.1 eV) at the metal-film interface, a complex of NH_3 or NO (399.6 eV) distributed throughout the passive film, and an ammonium salt (401.5 eV) observed at the passive film-solution interface.

TABLE OF CONTENTS

INTRODUCTION

Several studies have indicated that the addition of nitrogen to austenitic stainless steels can lead to improvements in passivation and pitting resistance(1-10). By far the greatest effect of nitrogen addition has been observed in Mo bearing stainless steels, suggesting a possible synergism between Mo and N(6-10). However, the apparent synergism between Mo and N may be due to the direct interaction of Mo and N or to N modifying the well known synergism between Cr and Mo.

In an initial characterization of the electrochemical behavior of 18-8 stainless steels containing between 0.04-0.24% N in deaerated 0.5M H_2SO_4 + 0.5M NaCl solution, Eckenrod and Kovach(3) observed that increasing the nitrogen content resulted in a significant reduction in the critical and passive current densities, and an increase in both pitting potential and passive range of potential. A small but significant increase in passivation potential was also observed.

Using samples of the 18-8-0.24% N alloy previously used by Eckenrod and Kovack(3), we have employed XPS to determine the role of N in the passive films formed in the 0.5M H_2SO_4 + 0.5M NaCl solution. We have also performed polarization studies of the 18-8-0.24% N alloy in deaerated 0.1M HCl solution.

EXPERIMENTAL

The compositions of the two alloys studied in this work are given in Table 1. The samples for XPS (7x10x1mm) were sealed in an evacuated quartz tube and annealed at 1060°C for 24 hours followed by a water quench, carried out by breaking the quartz tube in the water. The samples were ground with 240 grit and 600 grit silicon carbide and then subsequently polished with 6 micron and .25 micron diamond polish respectively.

Polarization was carried out in a conventional Greene cell using 0.5M H_2SO_4 + 0.5M NaCl or 0.1M HCl which was deaerated by purging with Ar for 2 hours. All potentials were measured against a saturated calomel electrode (S.C.E.). Specimens were cathodically treated for 15 min at -600 mV to reduce the polish formed oxide film. The specimens were potentiodynamically polarized in the anodic direction at 1 mV/sec to obtain polarization traces. Samples were also treated potentiostatically in 0.5M H_2SO_4 + 0.5M NaCl at 0 mV for 10 seconds or 1 hour in order to grow a passive film. Samples were extracted and washed with deaerated, doubly distilled water, then dried in argon and mounted onto the XPS probe. The entire operation was carried out in an Ar purged glove-box. The samples were transferred under argon to the specimen chamber which was also filled with Ar.

All XPS measurements were performed with a V.G. Scientific ESCA 3 MK II controlled by a V.G. Scientific Data System 1000. The system was equipped with an hemispherical analyser. An AlKα1,2 (1486.6 eV) source was used for XPS and operated at 400 watts. The sample was frozen by liquid nitrogen to prevent deterioration. The base pressure was approximately 2×10^{-9} torr. All XPS measurements were carried out at high (50^{o}) and low (20^{o}) photoelectron take-off angles, which were measured with respect to the plane of the sample, in order to observe the inner and outer layer of the film respectively (11). All XPS spectra reported in this paper were taken from narrow scans with the spectrometer's analyser set at 20 eV pass energy. For reference, the binding energy of the Au 4f7/2 line was found to be 83.8 eV with a FWHM of 1.4 eV. XPS spectra were corrected for the charge shifting by taking the carbon 1s spectrum at 284.6 eV.

All data were smoothed, utilizing a 9 or 21 point quadratic/cubic least squares program following the method developed by Savitsky and Golay (12) which was modified by Sherwood to cover the truncation errors at the ends of the spectra. Since the Cr 2p1/2 peak produces a AlKα3,4 satellite on the high binding energy side of the Cr 2p3/2 peak, a satellite subtraction program dependent on the analyser pass energy was used to eliminate the Cr 2p1/2 satellite. For peak synthesis, shape parameters included the peak's Gaussian/Lorentzian ratio

and tail characteristics which are height, slope and exponential to linear tail mix (13). The results given are of a semi-quantitative nature and are qualitatively typical of many spectra obtained throughout this study under various conditions.

RESULTS AND DISCUSSION

Electrochemical Studies

The polarization behavior of the 0.04 and 0.24% N stainless steels in both 0.5M H_2SO_4 + 0.5M NaCl and 0.1M HCl solutions is given in Figure 1 and the salient electrochemical characteristics in Table 2. It is apparent from Figure 1 and Table 2 that the data obtained in the acidic $SO_4^=/Cl^-$ solution agrees well with the earlier work of Eckenrod and Kovach(3).

A polarization study in deaerated 0.1M HCl, resulted in a generally inferior resistance to pitting and, in addition, we noted that the increase in N content had a much smaller effect on pitting resistance and raises the passivation potential significantly. In particular we note that for alloys of 0.04% and 0.24% N, the breakdown potentials in the $SO_4^=/Cl^-$ solution are higher than for the 0.1M HCl solution. This is a surprising result, since the highest resistance for pitting is observed in the more acidic (pH 0.4 compared to 1.2) solution having a higher Cl^- content. Therefore, it would appear that both $SO_4^=$ and N are responsible for the improvement in pitting resistance. In order to elucidate the role of $SO_4^=$ and N, XPS analysis of the highest N alloy (0.24% N) was performed following potentiostatic polarization in deaerated 0.5M H_2SO_4 + 0.5M NaCl solution at 0 mV

Table 1: Composition of 18-8 N Alloys (wt.%)

Alloy	Composition									
	C	Mn	P	S	Si	Ni	Cr	Mo	Cu	N
18-8-.04 N	0.053	1.77	0.031	0.008	0.41	8.49	19.27	0.36	0.16	0.04
18-8-.24 N	0.09	1.74	0.030	0.007	0.39	8.59	18.80	0.36	0.16	0.24

Table 2: Salient Electrochemical Characteristics

	E_{corr} (mV)	E_{pp} (mV)	I_{crit} (μAcm^{-2})	I_{pass} (μAcm^{-2})	$E_{pit(1st)}$ (mV)	$E_{pit(2nd)}$ (mV)	$E_{inhibit}$ (mV)
			0.5M H_2SO_4 + 0.5M NaCl pH 0.4				
18-8-.24N	-415.2	-304	1180	4.46	448	640	540
18-8-.04N	-415.6	-269	1641	8.41	448	-	-
			0.1M HCl pH 1.2				
18-8-.24N	-347.5	-179	71.57	4.47	340	-	-
18-8-.04N	-354.3	-259	45.0	4.10	200	-	-

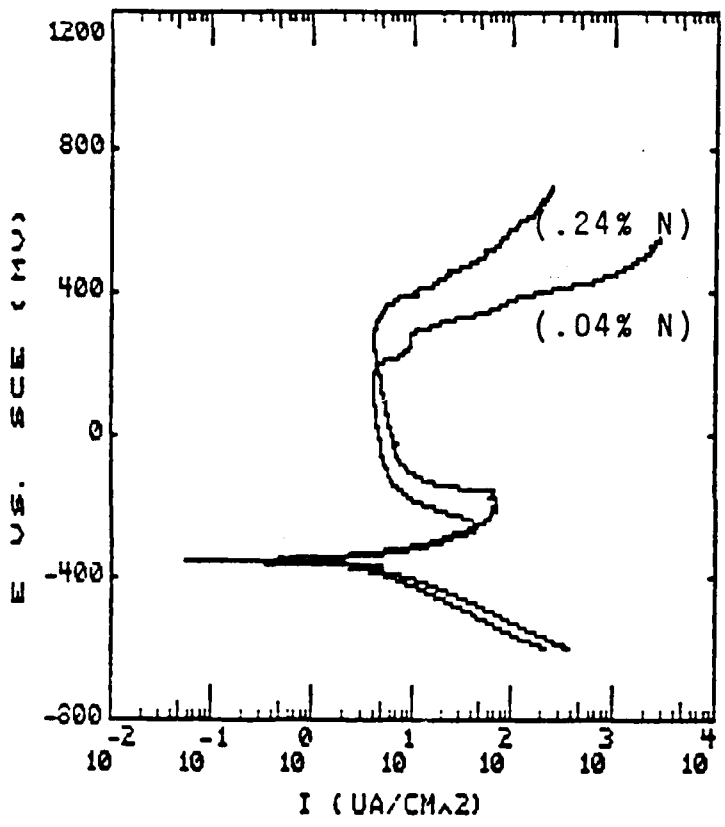

0.1M HCl
pH 1.2

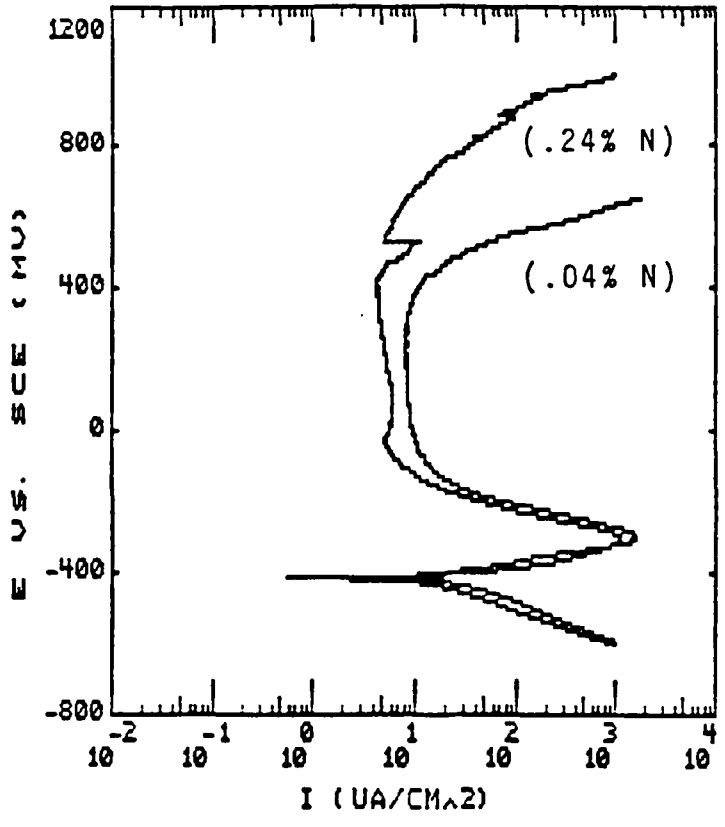

0.5M H_2SO_4 + 0.5M NaCl
pH 0.4

Fig. 1. Potentiodynamic polarization plots

for 10s and 1h. The 10s treatment was intended to reveal evidence of the earliest stages of passivity while the 1h treatment was intended to be representative of the fully developed passive film.

General Interpretation of High Resolution X-ray Photoelectron Spectra.

Selected spectra of N are presented in Figure 2. To aid in the comparison of 20 and 50 degree spectra, we have presented in Table 3 the peak areas for each of the main spectra obtained from the two passive films studied under the same instrumental conditions. The peak areas were normalized to 100 scans. This semiquantitative analysis provides a convenient guide to the relative abundance of various species in the inner and outer regions of the passive films. No attempt was made to convert peak areas to atomic percentages.

By considering the peak area ratios for each of the species in turn, for photoelectron take-off angles of 20 and 50 degrees, it is possible to provide an approximate description of the compositional variations throughout the passive film. Comparison is only made between photoelectron peaks representative of the photoelectrons of similar mean free path.

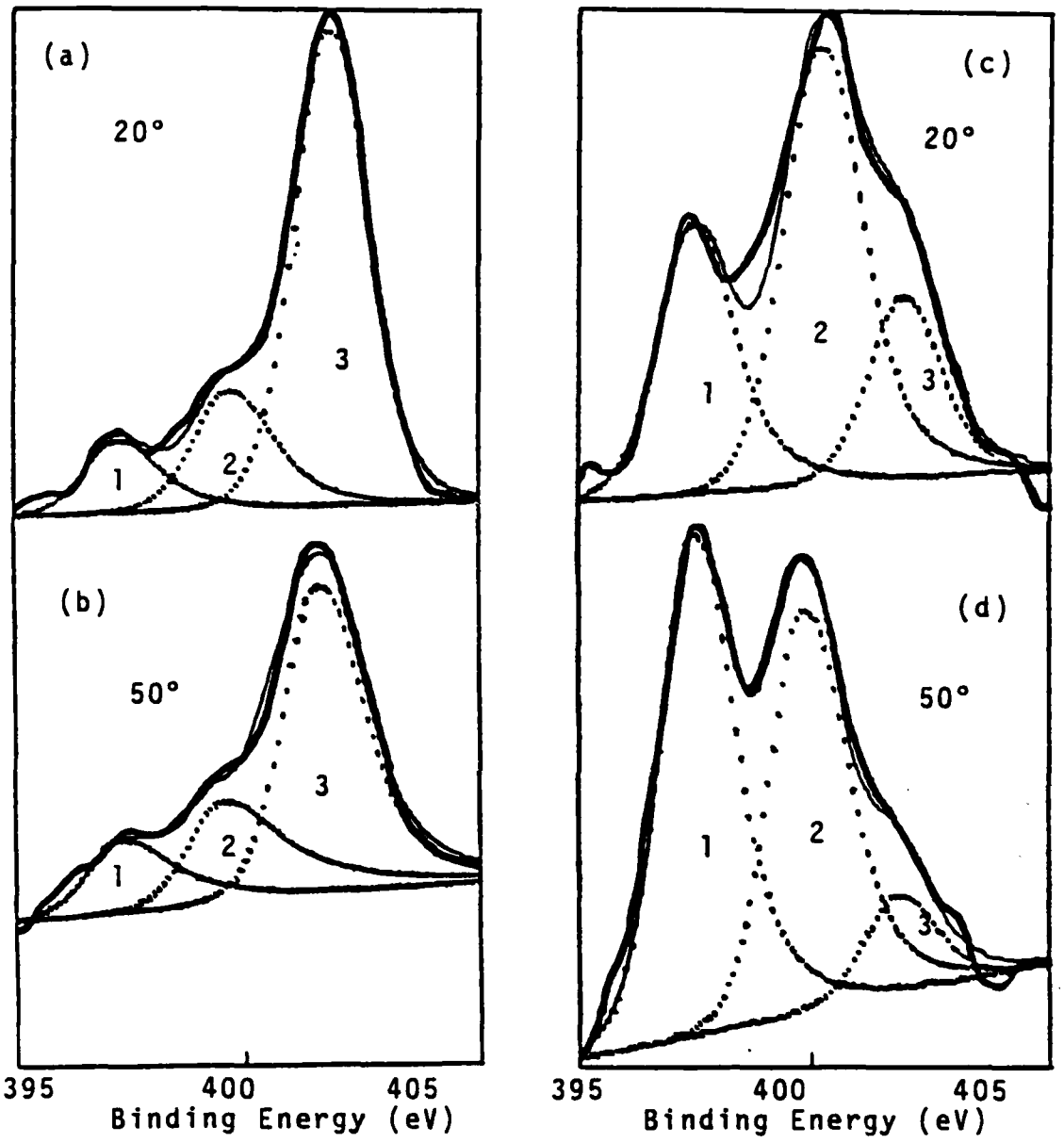

Fig. 2. N 1s photoelectron spectra obtained from the 10 second (curves a and b) and 1 hour (curves c and d) passive films at 0 mV (SCE) in deaerated 0.5M H_2SO_4 + 0.5M NaCl. 20° and 50° photoelectron takeoff angles are shown. The heavy lines are the original spectra and lighter lines, the fitted. Peak 1: Nitride 397.1±0.2 eV; Peak 2: NH_3 399.6±0.2 eV; Peak 3: NH_4^+ 401.5±0.2 eV.

Table 3. Integrated peak areas for the main spectra obtained from 10 sec. and 1 hr. passive films polarized at 0 mV in 0.5 M H_2SO_4 + 0.5 M NaCl.

			Integrated Peak Areas (x 1000)			
		Binding Energy (eV)	10 s. film 0 mV		1 hr. film 0 mV	
			20°	50°	20°	50°
Cr 2p	Cr(metal)	574.1	34.8	88.9	112.6	299.2
	Cr_2O_3	576.3	34.5	43.5	190.7	302.3
	$Cr(OH)_3$	577.0	91.2	127.8	378.8	490.7
	CrO_3	578.1	13.3	16.9	56.0	92.7
	$CrO_4^=$	579.3	12.8	13.9	46.9	49.0
Fe 2p	Fe(metal)	706.8	109.1	273.0	541.2	1228.0
	Fe^{2+}	709.3	24.3	31.4	204.3	282.6
	Fe^{3+}	711.3	12.5	20.4	63.4	100.4
N 1s	N(*nitride*)	397.1	4.3	5.9	9.0	23.6
	NH_3	399.6	7.7	8.6	14.7	18.9
	NH_4^+	401.5	28.7	24.0	5.7	4.3
O 1s	$O^=$	529.9	45.8	56.7	323.2	493.6
	OH^-	531.4	159.5	257.1	767.9	992.3
	H_2O	533.0	70.9	156.8	142.5	175.1
	$SO_4^=$	532.0	470.9	395.8	397.3	404.2
Ni 2p	Ni(metal)	852.3	22.7	36.6	98.3	172.9
Cl 2p	Cl^-	198.5	15.9	20.0	78.5	98.8

The technique has the advantage of being virtually non-destructive compared to ion milling. The disadvantage largely lay in problems associated with surface roughness and in the formation of diffuse interfaces and mixed phases. Our error is approximately 10 to 15 percent; this is based on inconsistancies that would result in our model, compared to previous work, if we considered changes less than 10 or 15%.

Cr 2p3/2 Spectra

Five components to the multiplet were found in each case corresponding to the following species:

a) Metallic Cr from the substrate

b) Cr^{3+} corresponding to Cr_2O_3

c) Cr^{3+} corresponding to $Cr(OH)_3$

d) Cr^{6+} corresponding to CrO_3

e) Cr^{6+} corresponding to CrO_4^{2-}

The films formed after 1 hour of polarization at 0 mV indicated stronger Cr_2O_3 and CrO_3 spectra at 50°, suggesting the formation of a mixed phase formed near to the metal film interface. $Cr(OH)_3$ and CrO_4^{2-} appears to be a mixed phase formed on top of the $XCr_2O_3 \cdot YCrO_3$ phase. Due to the semiquantitative nature of this analysis, specific X and Y values are currently not available. From the ratios of the peak areas for Cr_2O_3 and $Cr(OH)_3$, it seems that the proportion of Cr_2O_3 increases with

time of passivation at 0 mV. Metallic Cr was enriched in the substrate following each of the treatments. However, the greatest enrichment was observed following polarization at 0 mV for 10s.

Fe 2p3/2 Spectra

Three components to the multiplet were found in each case corresponding to:

a) Metallic Fe in the substrate

b) Fe^{2+}

c) Fe^{3+}

For each of the films studied the Fe^{2+} ion was the majority species. Each of the films showed a stronger contribution in the spectra from Fe^{2+} compared to Fe^{3+} at 20°, i.e. Fe^{2+} is enriched relative to Fe^{3+} in the exterior regions of the film. Relative to Cr and Ni, Fe appeared to be depleted in the substrate following each of the treatments.

Ni 2p3/2 Spectra

Only the metallic Ni spectra were recorded for each of the samples analysed. No evidence of oxidized Ni could be found. Ni appeared to be enriched in the substrate following both of the treatments.

Cl 2p Spectra

The Cl 2p spectra were enhanced at the high take-off

angle for each of the treatments, indicating that the Cl^- ion is not exclusively located in the outer region.

O 1s Spectra

Four components were clearly discernable:

a) O^{2-}

b) OH^-

c) H_2O

d) $SO_4^=$

N 1s Spectra

Three distinct N spectra were observed at the binding energies at 397.1 eV, 399.6 eV and 401.5 eV (Figure 2). From Table 4 of N 1s binding energies measured in this and other laboratories, it is apparent that spectra obtained at 397.1 eV corresponds to CrN. It is apparent from the literature that nitrogen atoms adsorbed on a series of transition elements tends to have binding energies typical of the bulk nitride(14,15). Thus, it cannot be determined from the recorded spectra whether a 2-dimensional or 3-dimensional nitride is formed during passivity. However, the binding energy is specific to CrN as opposed to Fe or Ni nitride (see Table 4). The N 1s spectra recorded at 401.5 eV closely corresponds to NH_4^+ as NH_4Cl or $(NH_4)_2SO_4$.

Table 4:
Nitrogen 1s Peak Positions
Data taken for C 1s=284.6 ± 0.2 eV

Compounds	Peak Position	Comments
Nitride/Fe	396.8 eV	attributed to N_2 reacted with Fe at 500°C. (15)
CrN	397.2 eV	compound (our data)
Nitride/Ni	397.7 eV	nitrogenized Ni (15)
NH_3	399.4 eV	adsorbed at 200 torr and measured at 0°C on Fe (15)
NO	399.6 eV	NO adsorbed at 200 torr on Ni and Fe substrate(14,15)
	400.6 eV	NO adsorbed at 1 torr on Fe substrate (15)
NH_4Cl	401.5 eV 401.3 eV	solid (18) solid (our data)
$(NH_4)_6Mo_7O_{24}$	401.5 eV	solid (our data)
NH_4^+	401.6 eV	attributed to NH_4FeSO_4 (15)
$\underline{NH_4}NO_3$	402.1 eV 401.7 eV	solid (18) solid (our data)
NH_2OH	402.4 eV	solid (our data)
$NaNO_2$	403.7 eV	solid (18)
NO_2^-	404.1 eV	on Ni substrate at 200 torr of NO (14)
NO_3^-	406.9 eV	Ni subsrate under 200 torr of N containing gasses (14)
$NH_4\underline{NO_3}$	407.1 eV 406.8 eV	solid (18) solid (our data)
$NaNO_3$	407.2 eV	solid (18)
$Cr(NO_3)_3$	407.2 eV	solid (our data)

The N 1s spectrum at 399.6 eV is not easily identifiable. Two species that may exhibit such a binding energy are adsorbed NH_3 (399.4 eV) and adsorbed NO (399.6 eV). We also note Hendrickson et al (16) have shown that the coordination of NH_3 to Co(III), Cr(III), Ir(III) and Rh(III) give partial ammonium like character to the ammonia group leading to a positive shift in the N 1s binding energy towards that of ammonium. The same authors have indicated that the magnitude of the positive shift in the N 1s binding energy for nitrosyl ligands of the NO^+ type is dependent on the back-bonding from the metal species into the NO^+ empty π^* orbital. The back-bonding is observed to be greatest for metals of low oxidation number and hence, the smallest positive shift in N 1s binding energy is observed for metals of lowest oxidation state. Thus, it is quite apparent that XPS cannot provide a positive identification of the N 1s spectra corresponding to 399.6 eV. It is, however, apparent from the variation of the intensity of the 399.6 eV spectra corresponding to the angle of photoelectron take-off, that the species is distributed throughout most of the passive film and therefore appears to be a complexing species of NH_3 or NO rather than a free ligand. However, the positive identification of NH_4^+ ions strongly suggests the possibility of an ammonia intermediate, or product of an NH_4^+ complexing reaction. We therefore assume that since NH_4^+ is clearly identified it is more probable that the N

1s spectra at 399.6 eV is due to NH_3 rather than NO.

The Nature of the Passive Film Found at 0 mV

By comparing the peak area ratios of Table 5. It is possible to determine the approximate location in the film of the various species. In Figure 3 we have provided schematic representations of the interpretation of the data provided in Table 5.

The schematics for the films formed at 0 mV after 10s and 1h passivation depict the relative displacement of four distinct regions. The 10s film exhibits an outer adsorption layer of Cl^- ions which appears to form on a layer enriched in NH_4^+ and $SO_4^=$. The main body of the film contains a mixture of Fe and Cr hydroxides and hydrated oxides. The appearance of NH_3 suggests the formation of NH_3 ligands probably associated with Cr and Fe. The variable angle spectra indicate that within this zone the outer region is richer in Fe^{2+} and OH^- and the inner region richer in Fe^{3+} and H_2O. An interfacial zone was formed consisting of a CrN layer over a Cr enriched substrate. Following 1h of passivation the film and substrate undergoes several changes. Firstly, it is seen from peak area intensities that the NH_4^+ and $SO_4^=$ species are reduced in concentration, and Cl^- ions have penetrated the NH_4^+, $SO_4^=$ layer. The main body of the film appears to develop a duplex structure with the formation of an

Table 5. Percentage change of integrated peak area ratios with change in photoelectron takeoff angle from 20° to 50° for 10 s. and 1 hr., 0 mV passive films.

Ratio	Percentage change from 20° to 50°	
	10 s. film 0 mV	1 hr. film 0 mV
$O^{=}/OH^{-}$	-23.2	+18.1
$O^{=}/H_2O$	-44.1	+24.2
$O^{=}/SO_4^{=}$ (O 1s)	+47.2	+50.1
OH^{-}/H_2O	-27.2	+5.1
$H_2O/SO_4^{=}$ (O 1s)	+163.1	+20.7
$OH^{-}/SO_4^{=}$ (O 1s)	+91.7	+27.0
nitride/NH_4^{+}	+64.0	+247.5
$NH_4^{+}/SO_4^{=}$ (O 1s)	-0.6	-25.9
nitride/NH_3	+22.8	+103.9
NH_3/NH_4^{+}	+33.5	+70.4
NH_3/H_2O	-49.5	+4.6
Cr_2O_3/NH_3	+12.8	+23.2
$Cr(OH)_3/NH_3$	+25.4	+0.7
$Cr_2O_3/Cr(OH)_3$	-10.1	+22.3
Cr_2O_3/nitride	-8.2	-39.6
$Cr(OH)_3$/nitride	+2.1	-50.6
Cr_2O_3/Fe^{2+}	-2.5	+14.5
Cr_2O_3/Fe^{3+}	-22.8	+0.1
$Cr(OH)_3/Fe^{2+}$	+8.4	-6.4
$Cr(OH)_3/Fe^{3+}$	-14.2	-18.2
Fe^{2+}/Fe^{3+}	-20.9	-12.7
$SO_4^{=}/Cl^{-}$ (S 2p)	+22.1	-5.4

Sign convention for percentage change of ratio X/Y:
positive %: species Y located above species X
negative %: species X located above species Y
(less than or equal to +/- 10-15% indicates species X and Y are located within the same spacial plane of the film)

Fig. 3. Schematic representations of the 10 s. and 1 hr., 0 mV passive films.

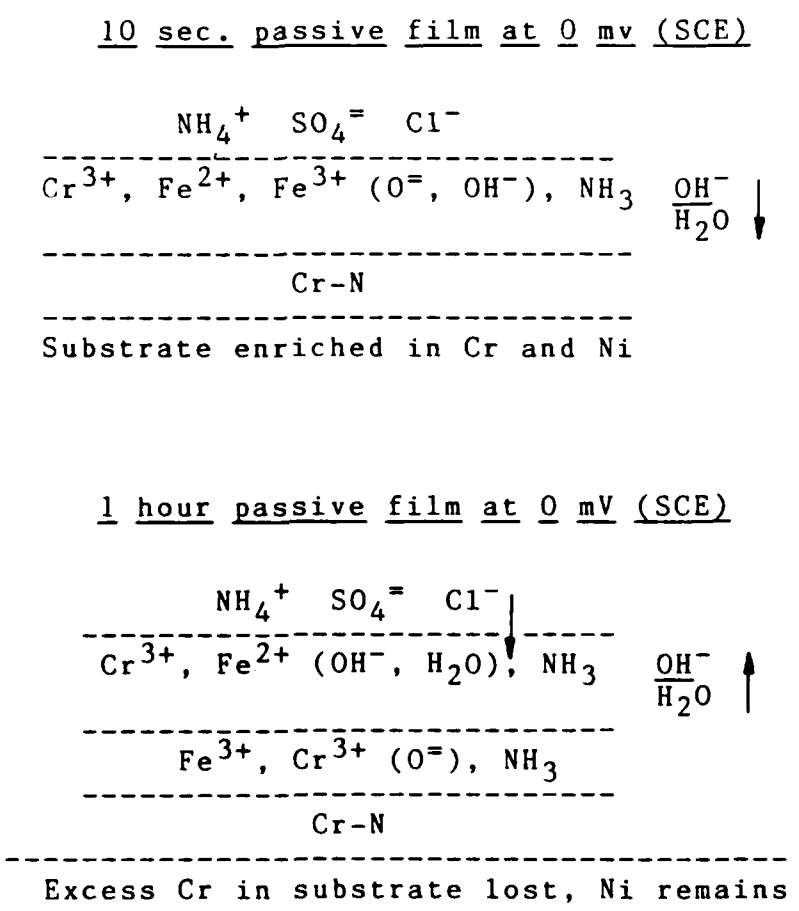

inner region consisting of oxides of Fe^{3+} and Cr^{3+} containing NH_3 groups. A further accumulation of CrN was also observed, while the substrate revealed a lowering in Cr content. While no evidence could be found of Ni in the passive film, Ni was found to become enriched in the substrate.

The formation of NH_4^+ at anodic potentials cannot take place by an electrochemical process, since the formation of NH_4^+ would require a reduction process. However, the accumulation of CrN, by selective dissolution of Fe, would provide a condition in which N acts as an electron acceptor. We propose that the chemical breakdown of the Cr-N bond by a polar solvent, such as H_2O, would render the Cr cation available for hydration and the nitrogen anions for protonation to NH_4^+, with perhaps NH_3 being formed as an intermediate product. The chemical formation of NH_4^+ would tend to lower local acidity thus aiding in the stabilization of a film of Fe and Cr hydroxides. A secondary effect of NH_4^+ formation also appears to be the formation of an ammonium sulfate salt layer, which may act as a temporary barrier between the metal and the solution. The salt layer appears to inhibit Cl^- ion attack, since pitting resistance is seen to be highest in the more acidic $SO_4^=/Cl^-$ solution. Thus, it would appear that the salt film protects the alloy from Cl^- ions and lowers the dissolution rate of the alloy, enabling a mixed hydroxide film to develop over a nitride layer.

Comparison of the N 1s spectra (Fig. 4) for the freshly polished surface and the cathodically treated surface show that NH_4^+ is not generated during the cathodic treatment as expected from the Pourbaix diagram (19) and the nitride is not totally reduced. This indicates that NH_4^+ is indeed formed chemically at anodic potentials as stated above. A shift of 0.7 eV to lower binding energy for the nitride peak position going from the polished surface (397.8 eV) to the cathodically treated surface (397.1 eV) is observed. In order to explain the observed difference in binding energy we suggest that adsorbed oxygen interacts with nitrogen at the metal-film interface of the polished surface. The presence of adsorbed oxygen would tend to withdraw the electron density from the less electronegative nitrogen, thereby increasing the bond strength between the nitrogen and Cr as shown by Kishi and Roberts (20). Identical binding energies were observed for the bulk nitrogen (397.1 eV) and the cathodically reduced surface.

The appearence of NH_3 in the passive film is perhaps surprising since ammonia complexes are highly soluble. It would therefore appear that some substitution of water ligands surrounding Cr or Fe with NH_3 has occurred during the formation of a highly hydrated passive film. The partial substitution of H_2O with NH_3 ligands would be expected to weaken the network structure of the passive film resulting from the deprotonation of

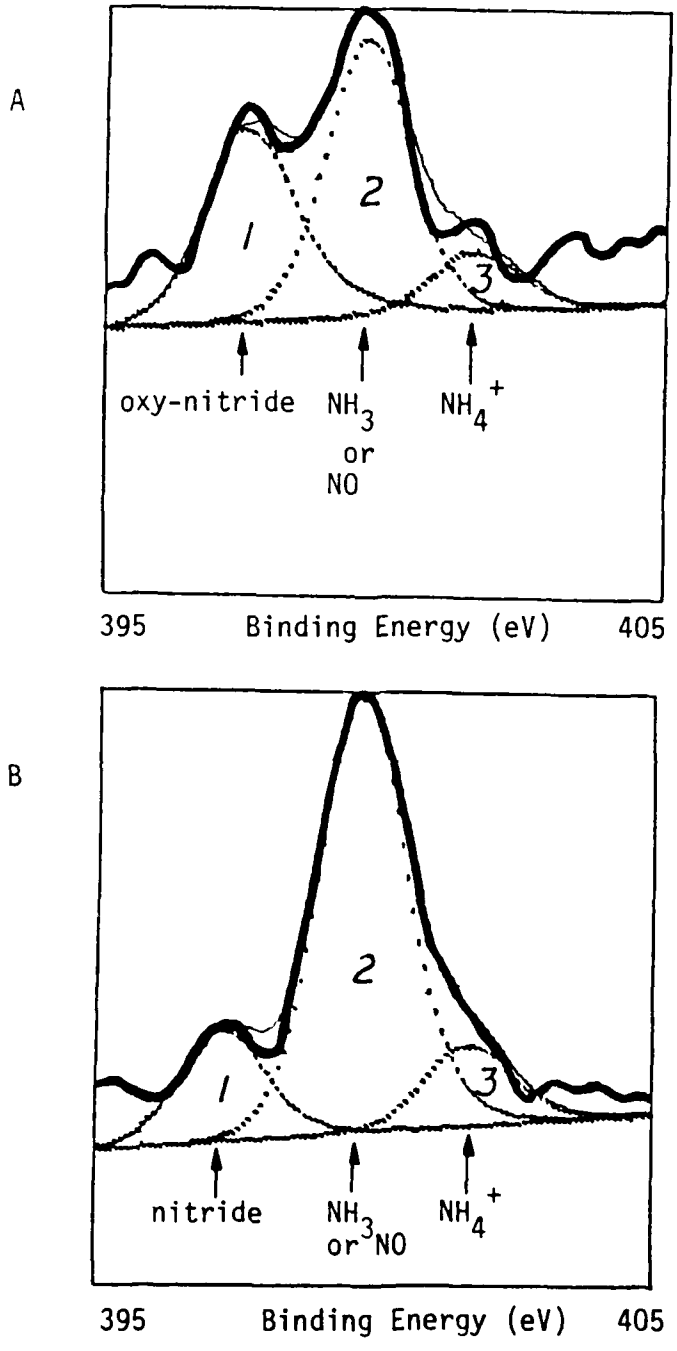

Fig. 4. N 1s photoelectron spectra from:
A: The freshly polished surface of the 0.24%N alloy.
B: The cathodically treated sprcimen at -600 mV for 15 min. in deaerated 0.5M H_2SO_4 + 0.5M NaCl.
The 50° photoelectron take-off angle is shown.

H_2O to form first OH^- and then $O^=$ bridges between cations.

The development of an inner oxide following Ih of passivation is a common behavior in stainless steels and appears to provide a diffusion barrier(17). The development of the nitride layer may thus serve both as a barrier layer and a rich source of nitrogen available to aid in the repassivation of active sites in the passive film.

CONCLUSIONS

1) Increasing the addition of N to an 18-8 stainless steel from 0.04 to 0.24% N has been shown to be effective in improving the pitting resistance in both deaerated solutions of 0.1M HCl (pH=1.2) and 0.5M H_2SO_4 + 0.5M NaCl (pH=0.4).

2) In general it appeared that N alloying was most effective in the presence of $SO_4^=$.

3) XPS analysis of passive films formed at 0 mV in the $SO_4^=/Cl^-$ solution after polarization of 10s and 1h indicated three major forms of combined N: a) CrN at the metal-film interface b) a N bearing complex. probably NH_3 within the film and c) NH_4^+ apparently associated with $SO_4^=$ concentrated at the passive film-solution interface.

4) The formation of NH_3 and NH_4^+ at anodic potentials suggests a chemical rather than electrochemical mechanism of formation.

5) Strong signals of NH_4^+ and $SO_4^=$ in the 10s film suggest that N aids in the repassivation process in two ways 1) by forming NH_4^+ the local acidity is reduced 2) by forming a $SO_4^=$ salt layer a hydrated Cr and Fe passive film may become established underneath.

ACKNOWLEDGEMENTS

We gratefully acknowledge the financial support of this research from the ONR (Dr. A.J. Sedriks, contracting officer) under contract N0001485 K0437. We also thank Dr. J.J. Eckenrod of Colt Industries for supplying the steel samples.

REFERENCES

1. Streicher, M.A., J. Electrochem. Soc.,Vol. 103, No. 7, p.375-90, (1956).
2. Uhlig, H.H, Trans. ASM, Vol. 30, p.947-80, (1942).
3. Eckenrod, J.J., Kovack, C.W., ASTM Spec. Tech. Publ. STP., 679, p. 17-41, (1977).
4. Kolotyrkin, Ya.M., Stepanov, I.A., Knyazheva, V.M., Babich, S.G., Int. Cong. on Metall. Corrosion, Vol. 1, p 258, Toronto, June 1984.
5. Osozawa, K. et al, Corros. Eng. (BOSHOKU GIJUZU), 24, 1, (1975).
6. Truman, J.E., Coleman, M.J., Pirt, K.R., Br. Corros. J., 12, p. 236, (1977).
7. Bandy, R. Van Rooyen, D., Corrosion, Vol. 39, No. 6, p. 227 (1983).
8. Lukina, O.I. et al, Zasheh. Met., Vol. 115, No. 5, p. 545 (1979).
9. Sedriks, A.J., Int Metal. Reviews, 28, No. 5, p. 306 (1983).
10. Lu, Y.C., Bandy, R., Clayton, C.R., Newman, R.C., J. Electrochem. Soc., 130, 1774, (1983).
11. Castle, J.E., Clayton, C.R., Corrosion Sci., 16(7) (1977).
12. Savitsky, A., Golay, M.J.E., Analytical Chemistry, 36, 8, 1627 (1964).

13. Sherwood, P.M., Practical Surface Analysis, Eds. D. Briggs and M.P. Seah, John Wiley & Sons, Ltd., New York (1983) p 445.

14. Honda, F.,Hirokawa, K., J. Electron Spect. & Rel. Phenon. 10(1977) 125-136

15. Honda, F., Hirokawa, K., ibid, 12(1977) 323-334

16. Hendrickson, D., Hollander, J.M., Jolly, W.L., Inorg. Chem., 8, p. 2642, (1969).

17. Brooks, A.R., Clayton, C.R., Doss K.G.K., Lu, Y.C., J. Electrochem. Soc., (in Press).

18. Burger, K., Taschismarov, F., Ebel, H., J. Electron Spect. & Rel. Phenon., 10(1977) 461-465.

19. Pourbaix, M., Atlas of Electrochemical Equilibria in Aqueous Solutions, Pergamon Press, Oxford (1966), p.493.

20. Kishi, K., Roberts, M.W., Surface Science, 62, 252, (1977).

END

10-86

DTIC